12096 *Biochemistry* **2009,** *48,* 12096–12103
DOI: 10.1021/bi9013819

BIOCHEMISTRY
including biophysical chemistry & molecular biology
Article

SDS Micelles as a Membrane-Mimetic Environment for Transmembrane Segments[†]

David V. Tulumello and Charles M. Deber*

Division of Molecular Structure and Function, Research Institute, Hospital for Sick Children, Toronto, Ontario, Canada M5G 1X8, and Department of Biochemistry, University of Toronto, Toronto, Ontario, Canada M5S 1A8

Received August 9, 2009; Revised Manuscript Received November 17, 2009

ABSTRACT: An inherent dilemma in the study of the structural biology of membrane proteins is that it is often necessary to use detergents to mimic the native lipid bilayer environment. This situation is of particular interest because the generation of high-resolution structures (through X-ray crystallography and solution NMR) has overwhelmingly relied upon identification of detergents in which membrane proteins may be solubilized without denaturation into a nonbiological state. While sodium dodecyl sulfate (SDS) is perhaps the most widely employed micelle-forming detergent for laboratory procedures involving membrane proteins, it has generally been regarded as a "harsh" detergent synonymous with membrane protein denaturation. Here we investigate systematically the SDS-solubilized states of a series of model α-helical transmembrane (TM) segments of varying Ala and Ile content in conjunction with selected single-Asn polar substitutions. Using Lys-tagged peptides typified by KKKKK-FAIAIAIIAWAIAIIAIAIAI-KKKKK in a series of circular dichroism, fluorescence, TOXCAT dimerization assay, and SDS−PAGE migration experiments, we find that both the local environment of the individual peptide helical surfaces and the formation of oligomeric states within the SDS−peptide complex are highly sensitive to point changes in peptide sequence, particularly with respect to local segment hydrophobicity and polar residue position. The overall results suggest that detergent micelles formed from SDS are largely capable of mimicking the tertiary interactions of protein-, lipid-, and aqueous-exposed helical surfaces that arise in the folded TM domains of proteins. The molecular characteristics of SDS−peptide complexes may thus portend a corresponding role for similar TM sequences in the in vivo assembly of polytopic membrane proteins.

Membrane proteins play essential roles in a variety of cellular processes such as signal transduction, solute transport, ion conductance, and catalysis, representing ~30% of the genes in most organisms (*1*) and the targets of ~70% of current drugs (*2*). Advances in understanding membrane protein folding have been made by considering their initial folding in two stages (*3*). In the first step, individual transmembrane (TM)[1] helices are inserted into the membrane by the translocon, a process largely dictated by a characteristic hydrophobic threshold (*4*). In the second step, individual TM helices associate via a combination of sequence-driven intramolecular and intermolecular helix−helix (TM−TM) interactions. Much progress has been made in identifying the latter protein−protein interactions, now known to include knobs-into-holes van der Waals packing, small-xxx-small motifs, aromatic stacking, and cation−π interactions (reviewed in ref *5*). Of further interest is the regular occurrence in TM segments of strongly polar residues (such as aspartic acid, glutamic acid, asparagine, and glutamine) that have been shown to promote oligomerization of model TM segments via side chain−side chain H-bonds and electrostatic interactions (*6*, *7*). In fact, TM segments contain an average of 20% polar residues (*8*), of which some likely act to stabilize or promote helix packing, while others participate in formation of central pores or channels for transport of ions or solutes.

Structural characterization of membrane proteins, particularly by crystallization and solution NMR techniques, has overwhelmingly relied upon their solubilization in detergent micelles (*9*−*11*). In reality, detergents are a more dynamic environment than the native bilayer and may impart flexibility and instability to the solubilized membrane protein, possibly resulting in denaturation (*9*, *12*, *13*). Among detergents considered "harsh" in this respect are anionic detergents such as sodium dodecyl sulfate (SDS). SDS is a well-characterized denaturant of soluble protein domains, doing so primarily by binding at hydrophobic sites and inducing a largely helical structure (*14*, *15*). This property indicates that SDS is not the detergent of choice for membrane protein crystallization, a process that necessarily relies upon protein−protein contacts of soluble domains (*9*). Charged detergents (including SDS), however, are often used in NMR studies where features of these micelles such as small size and good monodispersion are advantageous (*11*, *16*).

Although SDS has been used to denature polytopic membrane proteins (*13*), it is commonly employed in the identification of native helix−helix interactions in TM segments (*17*−*21*) and in

[†]This work was supported, in part, by grants to C.M.D. from the Canadian Institutes of Health Research (CIHR FRN-5810) and the Natural Science and Engineering Research Council of Canada (NSERC Discovery Grant A2807). D.V.T. is the recipient of an NSERC Doctoral Canadian Graduate Scholarship.

*To whom correspondence should be addressed: Division of Molecular Structure and Function, Research Institute, Hospital for Sick Children, 555 University Ave., Toronto, Ontario, Canada M5G 1X8. Telephone: (416) 813-5924. Fax: (416) 813-5005. E-mail: deber@sickkids.ca.

[1]Abbreviations: TM, transmembrane; SDS, sodium dodecyl sulfate; MW, molecular weight; CAT, chloramphenicol acetyltransferase; GpA, glycophorin A; PAGE, polyacrylamide gel electrophoresis; CD, circular dichroism spectroscopy; MRE, mean residue ellipticity; CMC, critical micelle concentration; ANS, 1-anilino-8-naphthalenesulfonate; FRET, Förster resonance energy transfer.

 Published on Web 11/18/2009

some instances is able to maintain the native tertiary and quaternary structure of membrane proteins that lack significant extramembranous domains (*22*, *23*). This situation evokes questions regarding the sequence dependence and biophysical nature of the susceptibility of TM segments to denaturation versus maintenance of the native TM structure upon SDS solubilization, and indeed the very concept of "denaturation" of membrane proteins in membrane-mimetic environments such as SDS micelles.

To examine these phenomena in a systematic manner, we investigate here the SDS detergent-solubilized states of a variety of designed hydrophobic α-helical TM segments in conjunction with selected single and multiple polar substitutions within these segments. Our findings show that (i) the local environment of individual helical surfaces within the protein−detergent complex is highly sequence-dependent and (ii) the structural and oligomeric variations stabilized by SDS solubilization reflect those that may arise in the folded transmembrane domains of proteins.

EXPERIMENTAL PROCEDURES

Transmembrane Segment Prediction. Peptide sequences were queried for prediction as TM segments using TM Finder (*24*), TMHMM2 (*25*), Phobius (*26*), MemBrain (*27*), TOPPRED2 (*28*), SOSUI (*29*), and TOPCONS (*30*). All programs were run using default settings. Core segment hydrophobicity was also calculated for peptide segments in the absence of the terminal Lys residues based upon the sum of individual Kyte−Doolittle parameters (*31*), Liu−Deber parameters (*32*), White−Wimley ΔG values of water to octanol transfer (*33*), and ΔG values of biological insertion (*34*) (with position dependence).

Peptide Synthesis and Purification. Peptides were synthesized using standard Fmoc [*N*-(9-fluorenyl)methoxycarbonyl] chemistry (*35*) on a PAL-PEG-PS [4′-aminomethyl-3′,5′-dimethoxyphenoxyvaleric acid-poly(ethylene glycol)] polystyrene resin (Applied Biosystems) that produces an amidated C-terminus upon peptide cleavage. Peptides were labeled at the N-termini by incubating the resin-bound peptides with excess label [4-(dimethylamino)azobenzene-4′-sulfonyl chloride (dabsyl chloride) or 5-(dimethylamino)-1-naphthalenesulfonyl chloride (dansyl chloride)] under basic conditions overnight. Cleaved peptides were purified by reverse phase high-pressure liquid chromatography on a C4 preparative column (Phenomenex). Mass spectrometry was used to identify the molecular weight (MW) of the purified peptides. All peptides were lyophilized following purification, resuspended in ddH_2O, and stored in aliquots at −20 °C. Peptide concentrations were determined using amino acid analysis of SDS-solubilized samples performed by the Advanced Protein Technology Centre of the Hospital for Sick Children.

TOXCAT Assays. Expression vector pccKan, pccGpA-WT, along with *Escherichia coli* strain NT326, was kindly provided by D. Engelman (Yale University, New Haven, CT) (*36*). Construction of pccAI10-WT (AI_{10}) has been described previously (*37*). pccAI5-WT (AI_5) was produced using the same methods. Additional sequences were produced by mutating the AI_{10} and AI_5 construct using the QuikChange site-directed mutagenesis kit (Stratagene). The sequences of all constructs were confirmed using DNA sequencing.

Constructs transformed into NT326 cells were grown, prepared, and assayed for both the expression of the total construct and reporter gene, chloramphenicol acetyltransferase (CAT), as previously described (*37*). All CAT concentration values were normalized to expression levels of the construct and to CAT concentrations of glycophorin A (GpA). All measurements were performed in at least triplicate, and two tailed *t* tests, assuming equal variance, were performed using Excel. Constructs were also tested for insertion efficiency on the basis of the ability to grow on M9 minimal medium plates with 0.4% maltose as the only carbon source. To achieve this, NT326 cells transformed with each mutant were streaked onto the plates and incubated for 2 days at 37 °C (*36*).

Sodium Dodecyl Sulfate−Polyacrylamide Gel Electrophoresis (*SDS−PAGE*) *Analysis*. SDS−PAGE was performed using precast 12% acrylamide NuPAGE gels in MES buffer (Invitrogen) according to the manufacturer's protocols. Coomassie Blue staining was used for visualization of the peptides at higher concentrations, while silver stain (Invitrogen) was used to develop gels containing lower concentrations. Apparent molecular weights were estimated on the basis of migration rates of Mark12 molecular weight standards (Invitrogen) using NIH Image to measure distances. Relative gel migration rates were calculated as (estimated MW from gel)/(formula MW from sequence) × 100% and reported as a percentage of the formula MW.

Circular Dichroism Spectroscopy. Freshly thawed aliquots of peptides were diluted to a final concentration between 20 and 40 μM in 10 mM Tris-HCl buffer (pH 8.0), with or without 34.7 mM (w/v) SDS. Spectra were recorded in a 1 mm path length cuvette on a Jasco J-810 circular dichroism spectropolarimeter. All spectra were background subtracted and converted to mean residue molar ellipticity [MRE (degrees per square centimeter per decimole)].

Tryptophan Fluorescence Measurements. Freshly thawed aliquots of peptides were diluted to a final concentration of 10 μM in 10 mM Tris-HCl buffer (pH 8.0), with or without 8.7 mM (w/v) SDS. Fluorescence emission spectra of peptides were recorded on a Hitachi F-400 Photon Technology International C-60 fluorescence spectrometer at an excitation wavelength of 295 nm with a 2 nm slit width, and emission measured between 310 and 400 nm with a 4 nm slit width. All spectra were corrected for light scattering effects by subtraction of background and by the correction function of FELIX software provided by the manufacturer. Measurements were recorded at a lower concentration of SDS to decrease light scattering effects. This strategy improved the signal-to-noise ratio, allowing for the more accurate determination of emission wavelength maxima, but had no significant effect on the shape of the emission spectra (Figure S1 of the Supporting Information). To confirm that a concentration of 8.7 mM SDS remained in micellar form under the conditions used, the critical micelle concentration (CMC) of the buffer system was determined by 1-anilino-8-naphthalenesulfonate (ANS) fluorescence as previously described (*38*). The CMC was found to be 5.86 mM with a standard error of ±0.11 mM, consistent with a previously reported value (obtained in the same buffer) of 5.61 ± 0.93 mM (*38*). The addition of peptide did not significantly affect the CMC (Figure S2 of the Supporting Information).

Förster Resonance Energy Transfer (*FRET*). FRET experiments were performed in 10 mM Tris-HCl buffer (pH 8.0), with or without 34.7 mM (w/v) SDS. All samples were prepared from frozen aliquots of peptides in triplicate or quadruplicate. Separately labeled peptides were mixed from aqueous solutions prior to addition of detergent and then allowed to

A

Name	Sequence[a]
AI_{10}	KKKKK-F[6]AIAIAIIAWAI[17]AIIAIAIAI-KKKKK-NH_2
$AI_{10}I17N$	KKKKK-F[6]AIAIAIIAWAN[17]AIIAIAIAI-KKKKK-NH_2
AI_5	KKK-Y[6]AAAIAAIAWAI[17]AAIAAAIAA-KK-NH_2
AI_5I17N	KKK-Y[6]AAAIAAIAWAN[17]AAIAAAIAA-KK-NH_2

[a]Lys tags increase peptide solubility in water and are not expected to affect peptide stoichiometry (*42*).

B

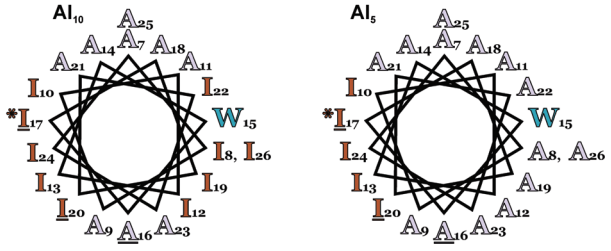

FIGURE 1: Design of model TM segments. (A) Sequences of peptides synthesized. AI_5 is numbered such that the first residue of TM sequence is the same as that in AI_{10} despite differing numbers of N-terminal Lys residues. (B) Helical wheel diagrams of the two parent peptides, AI_{10} and AI_5. Note that five residues on a single surface are substituted from Ile in AI_{10} to Ala in AI_5. The Ile-to-Asn substitution at position 17 (indicated by an asterisk) is located on the surface shared between these two peptides and is opposite of the Trp-15 residue. Residues that have previously been implicated in the formation of an antiparallel helix−helix interface within the context of covalently linked segments are underlined (*37*).

equilibrate at room temperature overnight. Dansyl emission spectra were recorded between 450 and 650 nm upon excitation at 341 nm. All spectra were background subtracted; the total fluorescence was integrated and reported as a value normalized to the mean emission of samples containing only the dansyl-labeled peptide.

RESULTS

Peptide Design and TM Insertion Prediction. To systematically investigate detergent solubilization of protein TM regions, we designed two categories of TM peptide segments consisting largely of Ala and Ile residues (sequences shown in Figure 1A). Both categories contain an identical surface capable, in principle, of forming helix−helix interactions in SDS through "knobs-into-holes" packing as well as via small-xxx-small (AxxxA) motifs, as elucidated in previous studies (*37*). The two groups of peptides differ primarily in that the more hydrophobic segment (AI_{10}) contains a total of 10 Ile residues while the less hydrophobic segment (AI_5) contains Ala residues instead of Ile residues at five sites that are positioned oppositely on a helical wheel from the ostensible interaction surface (Figure 1B). These changes, in turn, produce differences in net hydrophobicity and amphipathicity between the two prototypic segments. Variants of these two parent peptides were also produced in which a single Asn residue was introduced at position 17. This strategy produces an additional potential mode of interaction (side chain−side chain H-bonding) in the Asn-containing variants.

While all peptides were judged to be of sufficient hydrophobicity for membrane insertion on the basis of Kyte−Doolittle (*31*) and Liu−Deber (*32*) hydrophobicity scales, the least hydrophobic sequence (AI_5I17N) was deemed to moderately favor partitioning into less hydrophobic phases on the basis of the White−Wimley scale (*33*) and the Hessa et al. biological scale (*34*) (the ΔG of insertion into the more hydrophobic phase was between 1.0 and 0 kcal/mol). We noted that the inconsistent categorization among the scales of the Trp residue as being either "favorable" or "unfavorable" for membrane insertion produced the bulk of the variation in estimations of TM peptide hydropathy. The AI_5I17N sequence was also not identified as a TM segment by two of eight TM prediction programs [the Phobius (*26*) or TOPSCON (*30*) prediction programs did not predict a TM topology]. This latter sequence is thus representative of TM segments that are near the threshold for in vivo membrane insertion as dictated by the net hydrophobicity of the core sequence. We therefore expect the sets of peptides studied here to reflect the range of hydropathy characteristic of a natural variety of native TM segments.

Table 1: TOXCAT Measurement of Association of TM Segments in the *E. coli* Inner Membrane

TM segment	normalized[a] CAT concentration (standard deviation)
GpA	1.00 (0.04)
−TM[b]	0.02 (0.01)
AI_{10}	0.72 (0.17)
$AI_{10}I17N$	3.80 (0.99)
AI_5	0.50 (0.11)
AI_5I17N	0.16 (0.01)

[a]Mean levels of CAT expression have been normalized to relative expression levels of individual constructs and then to mean CAT expression levels obtained from glycophorin A (GpA). [b]−TM is a negative control in which the reporter construct contains a stop codon directly before the position where the putative TM segment is inserted and represents baseline expression. See Experimental Procedures for assay details.

Oligomerization within Bacterial Membranes. To determine initially if the designed sequences were capable of insertion and/or oligomerization in a native bilayer, we utilized the TOXCAT assay (*36*) (Table 1). In this assay, a TM segment is expressed as a chimeric fusion protein situated between the DNA binding domain of ToxR (a dimerization-dependent transcription factor) and the maltose binding protein (a monomeric periplasmic anchor). Upon expression of the construct, self-association of the TM segment results in the ToxR-driven activation of a reporter gene encoding chloramphenicol acetyltransferase (CAT), with the level of CAT expression being proportional to the strength of helix−helix interactions. We found that the more hydrophobic (AI_{10}) sequence formed an oligomer with normalized CAT expression levels that were ~70% of that of GpA, a known strong TM dimer. The mean level of CAT expression of the less hydrophobic sequence (AI_5) could not be distinguished statistically from AI_{10} ($p = 0.11$), indicating that the helix−helix interface is largely maintained within the native bilayer following Ile-to-Ala substitutions. Importantly, the addition of Asn to the more hydrophobic sequence ($AI_{10}I17N$) increased the relative level of CAT expression to ~3.5 times that of GpA, a large signal that may be due to higher-order (than dimer) oligomer formation (*39*). In contrast, the corresponding inclusion of an Asn residue in AI_5 prevented efficient membrane insertion of this segment [as assayed by growth with maltose as the sole carbon source (see Experimental Procedures)], and CAT expression levels were decreased to a value of ~15% of that of GpA.

Effect of Polar Residue Substitutions on the Peptide Oligomeric State(s) in SDS. Having determined by the TOXCAT assay that the peptides presented here form stable oligomeric state(s) in bacterial membranes, we performed SDS−PAGE in a neutral-pH system, as shown in Figure 2. Many sequences corresponding to TM segments of native membrane proteins have been shown to retain their native

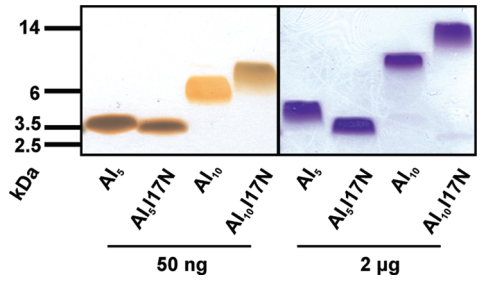

FIGURE 2: Oligomeric state(s) of model TM segment peptides. SDS−PAGE of peptides performed with a 12% NuPAGE precast gel. In the left panel, 50 ng of peptide was loaded in each lane and the gel was developed by silver staining. In the right panel, 2 μg of peptide was loaded in each lane and the gel was stained with Coomassie Blue.

oligomeric structure during SDS−PAGE experiments (*40*−*42*). Despite sharing an identical helical face shown by TOXCAT to be competent for helix−helix interaction in vivo, we found that the migration properties on SDS−PAGE of the two categories of TM segments (loaded with 2 μg) differ significantly (Figure 2, right panel). The more hydrophobic peptide (AI_{10}) runs primarily as an apparent dimer (apparent MW from R_f analysis is ~250% of its formula MW), while the less hydrophobic peptide (AI_5) migrates at a rate intermediate between the predicted monomer and dimer migration rates (~170% of its formula MW). The introduction of a single Asn residue into the common surface of the more hydrophobic peptide ($AI_{10}I17N$) slows the migration rate to one more consistent with a dimer−tetramer equilibrium (~360% of its formula MW), implying the creation of an additional helix−helix interface in this peptide. In contrast, the inclusion of an Asn residue in the less hydrophobic peptide at this same position (AI_5I17N) does not promote higher-order oligomer formation but rather increases the gel migration rate to ~140% of its formula MW. Faint bands (< 5% of the intensity of the main bands) with lower MWs in both AI_{10} (~120% of its formula MW) and $AI_{10}I17N$ (~90% of its formula MW) may represent monomeric forms or impurities in the sample.

We further observed that the migration rate on SDS−PAGE of two of the peptides, $AI_{10}I17N$ and AI_5, displayed a strong concentration dependence, with increased migration rates at lower peptide concentrations. This observation can be explained if these peptides exist in two oligomeric states that interconvert during the time course of the gel electrophoresis experiment. In this situation, only one band will be present during electrophoresis, positioned according to the average oligomeric state (*37*, *43*). A decrease in concentration will shift the equilibrium toward the smaller species, resulting in a decrease in the average oligomeric state and producing a faster migration rate. At much lower concentrations (50 ng of peptide loaded) (Figure 2, left panel), both AI_5 and AI_5I17N run with similar migration rates (~150 and 140%, respectively), both appearing as monomers, while AI_{10} and $AI_{10}I17N$ both migrate as dimers (~190 and 230%, respectively).

Oligomerization was also assessed using Förster resonance energy transfer (FRET) experiments. Peptides were labeled with dansyl (a fluorescence donor) or dabsyl (a fluorescence acceptor) moieties. Colocalization of oppositely labeled peptides within 30 Å (indicative of oligomerization) results in the transfer of energy from dansyl to dabsyl, decreasing the fluorescence intensity of the dansyl-labeled peptide. We found that the more hydrophobic peptide (AI_{10}) with and without an Asn displayed specific FRET in SDS buffer (Figure 3A), while peptides from the less hydrophobic series (AI_5) did not (Figure 3B), demonstrating

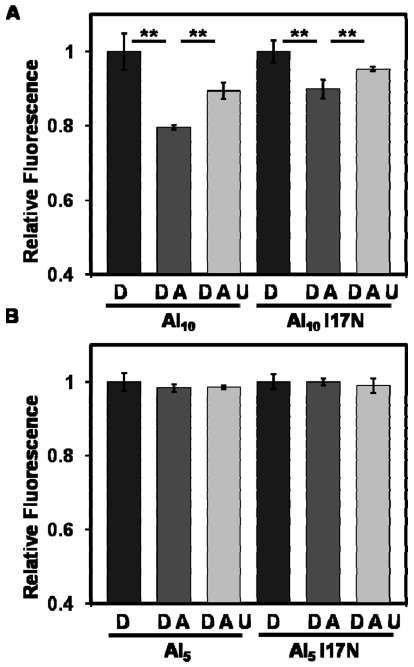

FIGURE 3: FRET experiments on TM peptides. FRET was performed in SDS buffer on (A) AI_{10} and (B) AI_5 peptides. The integration of the mean fluorescent signal of a minimum of three independent preparations is reported for each mixture of labeled peptides. Fluorescence is normalized to the mean of "donor only" samples. Donor only samples (D) contain 1 μM donor-labeled peptide and 1 μM unlabeled peptide. Donor/acceptor mixtures (DA) contain 1 μM donor-labeled peptide and 1 μM acceptor-labeled peptide. Donor/acceptor and unlabeled mixtures (DAU) contain 1 μM donor-labeled peptide, 1 μM acceptor-labeled peptide, and 4 μM unlabeled peptide. A decrease in fluorescence intensity upon addition of acceptor-labeled peptide (compare D to DA) indicates FRET between the two pairs. A subsequent increase in fluorescence upon inclusion of unlabeled peptide to the donor and acceptor mix (compare DA to DAU) indicates a decrease in the level of FRET, implying specific oligomerization. Error bars represent one standard deviation. Two-sided t tests were performed between D and DA as well as between DA and DAU assuming equal variance. Asterisks indicate $p < 0.01$.

that at the concentration used for FRET (2−6 μM total peptide), the latter peptides were not capable of forming an oligomer in SDS. The AI_5 series of peptides was further assayed for specific FRET under aqueous conditions, as they maintained a partially helical structure in the absence of detergent (see below); however, none was observed (data not shown).

Peptide Characterization by Circular Dichroism and Fluorescence Spectroscopy. To further assess the origin of the levels of peptide oligomerization in vivo versus detergent solubilization, we performed both circular dichroism (CD) and tryptophan fluorescence spectroscopy in aqueous buffer and in SDS. While CD spectra revealed that AI_{10} and $AI_{10}I17N$ were largely unstructured in aqueous buffer (Figure 4B), the AI_5 series had significant helical structure (as evidenced by strong negative peaks at 208 and 222 nm) due to both the increased Ala content [an aqueous α-helix promoter (*44*)] and the decreased Ile content (an aqueous β-sheet promoter) (Figure 4A). In media containing SDS, all peptides exhibited increased levels of helicity versus aqueous phase spectra (Figure 4), consistent with an essentially full helical structure (MRE at 222 nm near ~36000 deg cm^2 dmol^{-1}) (*45*, *46*). This is indicative of an uninterrupted hydrophobic helical span as observed in NMR studies of similar TM segments in detergents (*42*, *47*).

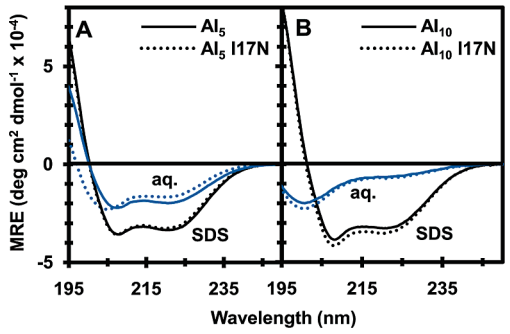

FIGURE 4: Circular dichroism of model TM segment peptides. Circular dichroism spectra were recorded for each of the model TM segments. Spectra of peptides in aqueous buffer are colored blue, while spectra obtained with addition of 34.7 mM SDS are colored black. AI_5 and AI_{10} spectra are depicted as solid lines and AI_5I17N and AI_{10}I17N spectra as dotted lines. (A) CD spectra of AI_5 peptides in SDS vs aqueous buffer. (B) CD spectra of AI_{10} peptides in SDS vs aqueous buffer.

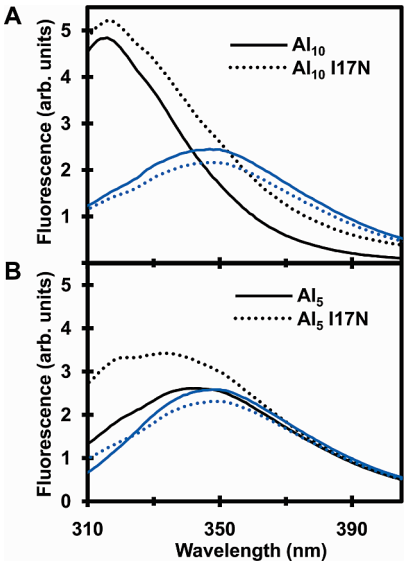

FIGURE 5: Tryptophan fluorescence of TM peptides. Tryptophan fluorescence spectra were recorded for each of the model TM segments. Spectra of peptides in aqueous buffer are colored blue, while spectra obtained with addition of 8.7 mM SDS are colored black. Excitation was performed at 295 nm, and emission was recorded between 310 and 400 nm. AI_5 and AI_{10} spectra are depicted as solid lines and AI_5I17N and AI_{10}I17N spectra as dotted lines. (A) Fluorescence spectra of AI_{10} and AI_{10}I17N peptides. (B) Fluorescence spectra of AI_5 and AI_5I17N peptides.

Tryptophan fluorescence spectroscopy demonstrated that the more hydrophobic peptides (AI_{10} and AI_{10}I17N) display a large blue shift in emission wavelength (31 nm) accompanied by an increase in intensity upon addition of SDS (Figure 5A), both of which are strong indicators of insertion of the central Trp residue into the core of a detergent micelle. In contrast, the less hydrophobic peptides both have comparatively smaller blue shifts (5 nm for AI_5 and 14 nm for AI_5I17N) and smaller increases in fluorescence intensity (Figure 5B). The observation that AI_5I17N displays a broader fluorescence emission spectrum in SDS compared to AI_5 with maximum intensity at a more blue-shifted position prompted us to examine this phenomenon in further detail. We synthesized a series of AI_5 analogues in which the position of insertion of the polar Asn residue was "walked" through the peptide sequence from N16 to N20. We also prepared an analogue that contained Asp instead of Asn at

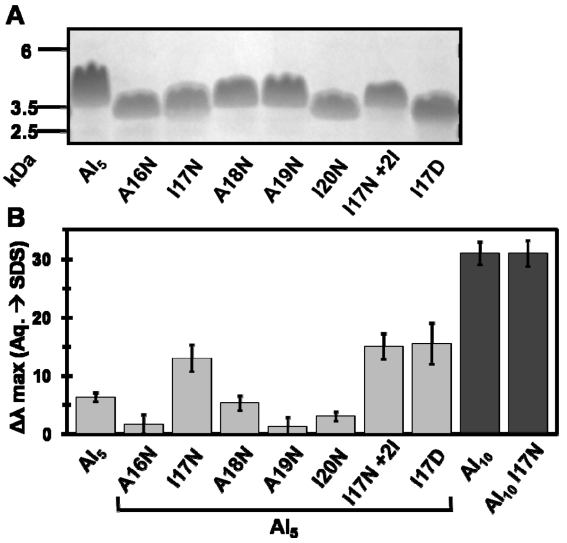

FIGURE 6: AI_5 peptides containing a polar substitution. (A) SDS–PAGE of a series of AI_5 peptides performed with a 12% NuPAGE precast gel. In each lane, 2 μg of peptides was loaded. (B) Changes in the Trp maximum emission wavelength of AI_5 peptides in SDS buffer vs aqueous buffer. Results with AI_{10} peptides are shown for comparison. Error bars represent the standard deviations of a minimum of three separate sample preparations.

position 17, and one that had hydropathy partially "restored" by conversion of Ala to Ile at positions 12 and 21 while Asn was retained at position 17. The results of SDS–PAGE analysis of this library are shown in Figure 6A. While there is some variation in migration positions on the gel that can be attributed largely to varying extents of SDS binding (*15*), all single-Asn analogues, and the Asp analogue, migrate faster than the AI_5 parent peptide, indicating their monomeric state. Finally, the set of fluorescence spectra we obtained for this library (Figure 6B) indicates that only substitutions at position 17 produce the relatively blue-shifted spectrum (including the 2I analogue), while AI_5 and AI_5 analogues with Asn at positions 16 and 18–20 display only a minor blue shift (~1–5 nm).

DISCUSSION

To preserve the native structure of a membrane protein, a detergent must be able to promote the retention of all native TM surfaces and interfaces. The increasing number of high-resolution membrane protein structures demonstrates that to a major extent, detergents have proven to be sufficient models of this situation (*48*). However, despite its common use throughout protein expression and purification procedures, SDS has not often been used for structural determinations [see, however, NMR studies (*11*, *16*)] and is primarily viewed as a harsh detergent and a denaturant. An improved understanding of the details of interactions of SDS with a variety of TM segments is thus essential to addressing the categorization of SDS as a TM domain denaturant versus a suitable membrane mimetic.

Structure of Peptide–Detergent Complexes. In the TM peptides studied here, both the more hydrophobic (AI_{10} series) and less hydrophobic (AI_5 series) peptides share an identical helical face designed to be competent for helix–helix interaction. Within this overall design, we nevertheless found that the inclusion of a polar Asn residue has opposing consequences for each segment, as deduced experimentally using SDS–PAGE gels, TOXCAT assays, CD spectroscopy, and Trp and FRET

fluorescence spectroscopy. Results from these combined studies indicate that in SDS micelles, AI_{10} forms a strong dimer (one locus of interaction), and upon addition of an Asn ($AI_{10}I17N$), a dimer−tetramer equilibrium is experienced during PAGE analysis (two loci of interaction). In contrast, AI_5 exists in a monomer−dimer equilibrium, but perhaps most intriguingly, the addition of an Asn (AI_5I17N) stabilizes the monomer form (no locus of interaction). Although both series contain much of the same potential for specific sequence-driven association, their SDS solvation states differ, in turn altering their helix−helix interactions. For the AI_5 series of peptides, a case can be made that with the reduced hydropathy of AI_5 versus AI_{10}, and with further reduction upon inclusion of a polar residue, the AI_5 peptides reside on average much closer to the effective micelle−water interface than the AI_{10} peptides do. This interpretation is supported experimentally by the observations that (i) the AI_5 series is predicted from several TM hydropathy scales to have only a moderate energetic preference between polar and nonpolar phases, (ii) AI_5I17N is a monomer, indicating that Asn-17 is not available for interhelical H-bond formation, (iii) TOXCAT assays support this largely monomer state (a manifest consequence of inefficient membrane insertion), and (iv) Trp blue shifts are >30 nm for the AI_{10} series, indicating complete "Trp burial" in the micelle. In contrast, blue shifts for the AI_5 series range from 1 to 5 nm for all peptides except those with Asn or Asp at position 17 (Figure 6B).

These results indicate the sequence dependence of the overall peptide−micelle structure and further suggest that the polar site specifically at position 17, occurring on the face directly opposite to the Trp-15 residue (Figure 1B), apparently "fixes" the Trp at a relatively micelle-buried position while the polar residue is drawn to the micelle−water interface. The broad fluorescence spectra displayed by the three N/D-17 peptides (as in Figure 6B) appear to indicate the existence of two (monomeric) states for these peptides, viz., one closer to and one farther from the effective water−micelle interface; this latter suggestion is supported by the observation of a shoulder on the principal peak in size exclusion chromatography performed in SDS (not shown).

Finally, while CD spectra of AI_{10}, $AI_{10}I17N$, AI_5, and AI_5I17N all exhibit comparable high helicity in SDS, we note that the Ala-rich peptides have high helicity in the aqueous phase versus the Ile-rich peptides (Figure 4), so that there is unlikely to be significant fraying of helices in any water-based portion(s) of the AI_5 segments that arise in the presence of micelles.

These experiments lead to the description of the structures of these peptides within the detergent micelles illustrated schematically in Figure 7. AI_{10} behaves according to the classical model of TM segment association within micelles, existing in a fully detergent-solvated state primarily as an oligomer (Figure 7A). While SDS induces an increased helical conformation in AI_5, it apparently does so without full solvation of side chains by the acyl detergent tails. In this case, the TM segment does not adopt the classical view of an α-helix inserted into the core of a micelle (Figure 7B) but instead has a surface exposed to a detergent headgroup or to the aqueous environment within the peptide−detergent complex (Figure 7C). This results in a decrease in the strength of the protein−protein interface [evidenced by the lack of dimerization during FRET (concentration of 2−6 μM) or during SDS−PAGE upon loading nanogram amounts (Figure 2, left panel)] as some fraction of the segment populates the water-interactive state, preventing full acyl tail solvation of the ostensible site of oligomerization. Such a model has been previously

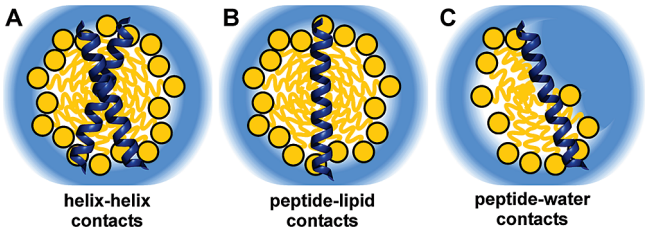

FIGURE 7: Peptide interactions within detergent micelles. Individual TM segments may exist in a variety of states in detergent micelles, as depicted schematically in panels A−C. (A) An oligomeric segment may have a surface with a preference to form tertiary interactions with another surface, effectively producing a protein−protein interface between interacting monomers. (B) A hydrophobic segment may have a strong preference for detergent solvation and exist as a monomer fully solvated by the acyl tails of the detergent. (C) A less hydrophobic surface or local subsegment arising within a TM-like segment may have a preference for aqueous solvation and partition to a state in which the segment is partially solvated by detergent headgroups and/or the surrounding aqueous environment.

reported in other TM segments BNIP3 (*20*) and GpA (*49*), where noninterfacial mutations that reduce hydrophobicity similarly decrease the apparent dimerization affinity in SDS. Thus, while the $AI_{10}I17N$ system likely forms a tight Asn−Asn side chain−side chain H-bond that produces a new helix−helix interaction interface along with higher-order oligomers, the introduction of I17N into the AI_5 system ultimately reduces the local hydrophobicity to the level at which partial aqueous solvation becomes the most stabilizing alternative.

Effectiveness of SDS as a "Membrane Mimetic". This study demonstrates that SDS can support TM helices as oligomeric species [i.e., the $AI_{10}I17N$ peptide displays both the highest oligomeric state(s) in SDS (Figure 2, right panel) and a correspondingly high TOXCAT signal (Table 1)], stabilize a micelle-solvated monomeric state, and/or support a state promoted by aqueous solvation of a local segment at the micelle−water interface. Importantly, the access to water available to a TM segment embedded in a micelle system (vs the absence of this possibility in a lipid bilayer without major structural rearrangement) may serve as a surrogate for the in vivo structures of many membrane proteins where helix−aqueous interactions that contribute directly to protein structure and function (i.e., pores, channels) span the TM domains of the proteins (*50*, *51*). Thus, where close-to-threshold hydrophobicity exists for a given TM sequence, introduction of a polar mutation into a protein- or lipid-exposed surface may induce a preference for an aqueous-exposed conformation (a change from panel B to panel C of Figure 7). The capacity of SDS to respond to such nuance of sequence as well as to peptide concentration mitigates against the typical view of denaturation by harsh detergents.

Our findings suggest that SDS solvation of transmembrane segments, particularly with sequence-specific preservation of helix−helix interactions and compatibility with aqueous-exposed regions, may in fact constitute a relevant biological model. The striking ability of the local SDS micellar environment to alter conformation and stoichiometry due to a single point mutation suggests that corresponding mutations in vivo can similarly impact local protein structure. The SDS-induced denaturation that is commonly observed for TM regions of proteins may in some cases be an allosteric consequence of the loss of native structure in extramembranous regions. Also, in SDS unfolding experiments there may not always be large conformational changes in TM

regions that correspond to a true unfolding transition (*13*). At least for membrane proteins with relatively short, stable extramembranous loops, our results suggest that SDS could largely preserve robust tertiary structure and, as such, serve as a useful mimic of protein structure within the hydrophobic core of a biological membrane.

SUPPORTING INFORMATION AVAILABLE

A figure comparing the Trp fluorescence spectra of peptides obtained in the presence of 8.7 and 34.7 mM SDS and a figure showing the ANS fluorescence experiments used to calculate the critical micelle concentration under the buffer conditions used, in the presence and absence of peptides. This material is available free of charge via the Internet at http://pubs.acs.org.

REFERENCES

1. Wallin, E., and von Heijne, G. (1998) Genome-wide analysis of integral membrane proteins from eubacterial, archaean, and eukaryotic organisms. *Protein Sci. 7*, 1029–1038.
2. Yildirim, M. A., Goh, K. I., Cusick, M. E., Barabasi, A. L., and Vidal, M. (2007) Drug-target network. *Nat. Biotechnol. 25*, 1119–1126.
3. Popot, J. L., and Engelman, D. M. (1990) Membrane protein folding and oligomerization: The two-stage model. *Biochemistry 29*, 4031–4037.
4. White, S. H., and von Heijne, G. (2008) How translocons select transmembrane helices. *Annu. Rev. Biophys. 37*, 23–42.
5. Rath, A., Tulumello, D. V., and Deber, C. M. (2009) Peptide models of membrane protein folding. *Biochemistry 48*, 3036–3045.
6. Zhou, F. X., Merianos, H. J., Brunger, A. T., and Engelman, D. M. (2001) Polar residues drive association of polyleucine transmembrane helices. *Proc. Natl. Acad. Sci. U.S.A. 98*, 2250–2255.
7. Gratkowski, H., Lear, J. D., and DeGrado, W. F. (2001) Polar side chains drive the association of model transmembrane peptides. *Proc. Natl. Acad. Sci. U.S.A. 98*, 880–885.
8. Stevens, T. J., and Arkin, I. T. (1999) Are membrane proteins "inside-out" proteins? *Proteins 36*, 135–143.
9. Prive, G. G. (2007) Detergents for the stabilization and crystallization of membrane proteins. *Methods (San Diego, CA, U.S.) 41*, 388–397.
10. Carpenter, E. P., Beis, K., Cameron, A. D., and Iwata, S. (2008) Overcoming the challenges of membrane protein crystallography. *Curr. Opin. Struct. Biol. 18*, 581–586.
11. Sanders, C. R., and Sonnichsen, F. (2006) Solution NMR of membrane proteins: Practice and challenges. *Magn. Reson. Chem. 44*, S24–S40.
12. le Maire, M., Champeil, P., and Moller, J. V. (2000) Interaction of membrane proteins and lipids with solubilizing detergents. *Biochim. Biophys. Acta 1508*, 86–111.
13. Renthal, R. (2006) An unfolding story of helical transmembrane proteins. *Biochemistry 45*, 14559–14566.
14. Imamura, T. (2006) Protein-Surfactant Interactions. In Encyclopedia of Surface and Colloid Science (Somasundaran, P., Ed.) pp 5251−5263, Taylor & Francis, New York.
15. Rath, A., Glibowicka, M., Nadeau, V. G., Chen, G., and Deber, C. M. (2009) Detergent binding explains anomalous SDS-PAGE migration of membrane proteins. *Proc. Natl. Acad. Sci. U.S.A. 106*, 1760−1765.
16. Page, R. C., Moore, J. D., Nguyen, H. B., Sharma, M., Chase, R., Gao, F. P., Mobley, C. K., Sanders, C. R., Ma, L., Sonnichsen, F. D., Lee, S., Howell, S. C., Opella, S. J., and Cross, T. A. (2006) Comprehensive evaluation of solution nuclear magnetic resonance spectroscopy sample preparation for helical integral membrane proteins. *J. Struct. Funct. Genomics 7*, 51–64.
17. Lemmon, M. A., Flanagan, J. M., Hunt, J. F., Adair, B. D., Bormann, B. J., Dempsey, C. E., and Engelman, D. M. (1992) Glycophorin A dimerization is driven by specific interactions between transmembrane α-helices. *J. Biol. Chem. 267*, 7683–7689.
18. Melnyk, R. A., Partridge, A. W., and Deber, C. M. (2001) Retention of native-like oligomerization states in transmembrane segment peptides: Application to the *Escherichia coli* aspartate receptor. *Biochemistry 40*, 11106–11113.
19. Therien, A. G., and Deber, C. M. (2002) Oligomerization of a peptide derived from the transmembrane region of the sodium pump gamma subunit: Effect of the pathological mutation G41R. *J. Mol. Biol. 322*, 583–590.
20. Sulistijo, E. S., and MacKenzie, K. R. (2006) Sequence dependence of BNIP3 transmembrane domain dimerization implicates side-chain hydrogen bonding and a tandem GxxxG motif in specific helix-helix interactions. *J. Mol. Biol. 364*, 974–990.
21. Gorman, P. M., Kim, S., Guo, M., Melnyk, R. A., McLaurin, J., Fraser, P. E., Bowie, J. U., and Chakrabartty, A. (2008) Dimerization of the transmembrane domain of amyloid precursor proteins and familial Alzheimer's disease mutants. *BMC Neurosci. 9*, 17.
22. Arkin, I. T., Adams, P. D., MacKenzie, K. R., Lemmon, M. A., Brunger, A. T., and Engelman, D. M. (1994) Structural organization of the pentameric transmembrane α-helices of phospholamban, a cardiac ion channel. *EMBO J. 13*, 4757–4764.
23. Chill, J. H., Louis, J. M., Miller, C., and Bax, A. (2006) NMR study of the tetrameric KcsA potassium channel in detergent micelles. *Protein Sci. 15*, 684–698.
24. Deber, C. M., Wang, C., Liu, L. P., Prior, A. S., Agrawal, S., Muskat, B. L., and Cuticchia, A. J. (2001) TM Finder: A prediction program for transmembrane protein segments using a combination of hydrophobicity and nonpolar phase helicity scales. *Protein Sci. 10*, 212–219.
25. Krogh, A., Larsson, B., von Heijne, G., and Sonnhammer, E. L. (2001) Predicting transmembrane protein topology with a hidden Markov model: Application to complete genomes. *J. Mol. Biol. 305*, 567–580.
26. Kall, L., Krogh, A., and Sonnhammer, E. L. (2004) A combined transmembrane topology and signal peptide prediction method. *J. Mol. Biol. 338*, 1027–1036.
27. Shen, H., and Chou, J. J. (2008) MemBrain: Improving the accuracy of predicting transmembrane helices. *PLoS One 3*, e2399.
28. von Heijne, G. (1992) Membrane protein structure prediction. Hydrophobicity analysis and the positive-inside rule. *J. Mol. Biol. 225*, 487–494.
29. Hirokawa, T., Boon-Chieng, S., and Mitaku, S. (1998) SOSUI: Classification and secondary structure prediction system for membrane proteins. *Bioinformatics 14*, 378–379.
30. Bernsel, A., Viklund, H., Falk, J., Lindahl, E., von Heijne, G., and Elofsson, A. (2008) Prediction of membrane-protein topology from first principles. *Proc. Natl. Acad. Sci. U.S.A. 105*, 7177–7181.
31. Kyte, J., and Doolittle, R. F. (1982) A simple method for displaying the hydropathic character of a protein. *J. Mol. Biol. 157*, 105–132.
32. Liu, L. P., and Deber, C. M. (1999) Combining hydrophobicity and helicity: A novel approach to membrane protein structure prediction. *Bioorg. Med. Chem. 7*, 1–7.
33. Wimley, W. C., Creamer, T. P., and White, S. H. (1996) Solvation energies of amino acid side chains and backbone in a family of host-guest pentapeptides. *Biochemistry 35*, 5109–5124.
34. Hessa, T., Meindl-Beinker, N. M., Bernsel, A., Kim, H., Sato, Y., Lerch-Bader, M., Nilsson, I., White, S. H., and von Heijne, G. (2007) Molecular code for transmembrane-helix recognition by the Sec61 translocon. *Nature 450*, 1026–1030.
35. Amblard, M., Fehrentz, J. A., Martinez, J., and Subra, G. (2005) Fundamentals of modern peptide synthesis. *Methods Mol. Biol. 298*, 3–24.
36. Russ, W. P., and Engelman, D. M. (1999) TOXCAT: A measure of transmembrane helix association in a biological membrane. *Proc. Natl. Acad. Sci. U.S.A. 96*, 863–868.
37. Johnson, R. M., Heslop, C. L., and Deber, C. M. (2004) Hydrophobic helical hairpins: Design and packing interactions in membrane environments. *Biochemistry 43*, 14361–14369.
38. Esposito, C., Colicchio, P., Facchiano, A., and Ragone, R. (1998) Effect of a weak electrolyte on the critical micellar concentration of sodium dodecyl sulfate. *J. Colloid Interface Sci. 200*, 310–312.
39. Johnson, R. M., Hecht, K., and Deber, C. M. (2007) Aromatic and cation-π interactions enhance helix-helix association in a membrane environment. *Biochemistry 46*, 9208–9214.
40. Wegener, A. D., and Jones, L. R. (1984) Phosphorylation-induced mobility shift in phospholamban in sodium dodecyl sulfate-polyacrylamide gels. Evidence for a protein structure consisting of multiple identical phosphorylatable subunits. *J. Biol. Chem. 259*, 1834–1841.
41. Heginbotham, L., Odessey, E., and Miller, C. (1997) Tetrameric stoichiometry of a prokaryotic K^+ channel. *Biochemistry 36*, 10335–10342.
42. Melnyk, R. A., Partridge, A. W., Yip, J., Wu, Y., Goto, N. K., and Deber, C. M. (2003) Polar residue tagging of transmembrane peptides. *Biopolymers 71*, 675–685.
43. Artemenko, E. O., Egorova, N. S., Arseniev, A. S., and Feofanov, A. V. (2008) Transmembrane domain of EphA1 receptor forms dimers in membrane-like environment. *Biochim. Biophys. Acta 1778*, 2361–2367.

44. Chou, P. Y., and Fasman, G. D. (1978) Empirical predictions of protein conformation. *Annu. Rev. Biochem. 47*, 251–276.
45. Chen, Y. H., Yang, J. T., and Chau, K. H. (1974) Determination of the helix and β form of proteins in aqueous solution by circular dichroism. *Biochemistry 13*, 3350–3359.
46. Manning, M. C., and Woody, R. W. (1991) Theoretical CD studies of polypeptide helices: Examination of important electronic and geometric factors. *Biopolymers 31*, 569–586.
47. MacKenzie, K. R., Prestegard, J. H., and Engelman, D. M. (1997) A transmembrane helix dimer: Structure and implications. *Science 276*, 131–133.
48. White, S. H. (2009) Biophysical dissection of membrane proteins. *Nature 459*, 344–346.
49. Duong, M. T., Jaszewski, T. M., Fleming, K. G., and MacKenzie, K. R. (2007) Changes in apparent free energy of helix-helix dimerization in a biological membrane due to point mutations. *J. Mol. Biol. 371*, 422–434.
50. Abramson, J., Smirnova, I., Kasho, V., Verner, G., Iwata, S., and Kaback, H. R. (2003) The lactose permease of *Escherichia coli*: Overall structure, the sugar-binding site and the alternating access model for transport. *FEBS Lett. 555*, 96–101.
51. Stroud, R. M., Miercke, L. J., O'Connell, J., Khademi, S., Lee, J. K., Remis, J., Harries, W., Robles, Y., and Akhavan, D. (2003) Glycerol facilitator GlpF and the associated aquaporin family of channels. *Curr. Opin. Struct. Biol. 13*, 424–431.